



An increase in surface hydrophobicity mediates chaperone activity in N-chlorinated RidA

Marharyta Varatnitskaya^a, Julia Fasel^a, Alexandra Müller^a, Natalie Lupilov^a, Yunlong Shi^b, Kristin Fuchs^{c,d}, Marco Krewing^e, Christoph Jung^{f,g}, Timo Jacob^{f,g,h}, Barbara Sitek^{c,d}, Julia E. Bandow^e, Kate S. Carroll^b, Eckhard Hofmannⁱ, Lars I. Leichert^{a,*}

^a Ruhr University Bochum, Institute of Biochemistry and Pathobiochemistry, Microbial Biochemistry, Bochum, Germany

^b UF Scripps Biomedical Research, Department of Chemistry, 130 Scripps Way, Jupiter, FL, 33458, USA

^c Ruhr University Bochum, Medical Proteome Center, Bochum, Germany

^d Klinik für Anästhesiologie, Intensivmedizin und Schmerztherapie, Universitätsklinikum Knappschaftskrankenhaus Bochum, Bochum, Germany

^e Ruhr University Bochum, Applied Microbiology, Faculty of Biology and Biotechnology, Bochum, Germany

^f Helmholtz Institute Ulm – Electrochemical Energy Storage, Basics of Electrochemistry, Ulm, Germany

^g Karlsruhe Institute of Technology (KIT), P.O. Box 3640, 76021, Karlsruhe, Germany

^h Institute of Electrochemistry, Ulm University, Albert-Einstein-Allee 47, D-89081, Ulm, Germany

ⁱ Ruhr University Bochum, Protein Crystallography, Bochum, Germany

ARTICLE INFO

Keywords:

N-Chlorination
Oxidation
Oxidative stress
E. coli
Chaperone

ABSTRACT

Under physiological conditions, *Escherichia coli* RidA is an enamine/imine deaminase, which promotes the release of ammonia from reactive enamine/imine intermediates. However, when modified by hypochlorous acid (HOCl), it turns into a potent chaperone-like holdase that can effectively protect *E. coli*'s proteome during oxidative stress. However, it is unknown, which residues need to be chlorinated for activation. Here, we employ a combination of LC-MS/MS analysis, a chemo-proteomic approach, and a mutagenesis study to identify residues responsible for RidA's chaperone-like function. Through LC-MS/MS of digested RidA_{HOCl}, we obtained direct evidence of the chlorination of one arginine residue. To overcome the instability of the N-chloramine modification, we established a chemoproteomic approach using 5-(dimethylamino) naphthalene-1-sulfinic acid (DANSO₂H) as a probe to label N-chlorinated lysines. Using this probe, we were able to detect the N-chlorination of six additional lysine residues. Moreover, using a mutagenesis study to genetically probe the role of single arginine and lysine residues, we found that the removal of arginines R105 and/or R128 led to a substantial reduction of RidA_{HOCl}'s chaperone activity. These results, together with structural analysis, confirm that the chaperone activity of RidA is concomitant with the loss of positive charges on the protein surface, leading to an increased overall protein hydrophobicity. Molecular modelling of RidA_{HOCl} and the rational design of a RidA variant that shows chaperone activity even in the absence of HOCl further supports our hypothesis. Our data provide a molecular mechanism for HOCl-mediated chaperone activity found in RidA and a growing number of other HOCl-activated chaperones.

1. Introduction

Phagocytosis is a crucial mechanism of our innate immune system used in the defense against and the elimination of pathogens, such as bacteria and fungi. Within the phagosome, a cellular compartment formed from the cytoplasmic membrane during phagocytosis, pathogens are exposed to a complex mixture of different reactive oxygen and nitrogen species, including superoxide radicals, hydrogen peroxide,

peroxynitrite, and hypochlorous acid (for comprehensive reviews see Refs. [1,2]).

Hypochlorous acid is produced by the heme enzyme myeloperoxidase from H₂O₂ and chlorine. HOCl is a highly reactive oxidizing and chlorinating agent and one of the most potent oxidants that exist in human cells [3]. It is known to cause a variety of modifications in virtually all cellular macromolecules including DNA [4], lipids [5–7], carbohydrates [8], and proteins. Amino acid modifications caused by

* Corresponding author.

E-mail address: lars.leichert@ruhr-uni-bochum.de (L.I. Leichert).

<https://doi.org/10.1016/j.redox.2022.102332>

Received 23 March 2022; Received in revised form 29 April 2022; Accepted 4 May 2022

Available online 7 May 2022

2213-2317/© 2022 The Authors. Published by Elsevier B.V. This is an open access article under the CC BY license (<http://creativecommons.org/licenses/by/4.0/>).

HOCl include oxidation of cysteine and methionine residues and chlorination of tyrosine, lysine, arginine, and histidine [9,10]. Often these modifications are irreversible, leading to protein misfolding and aggregation [11–13], loss of function, and eventual degradation by proteolytic enzymes [11]. Thus, modification of proteins by oxidative stressors and HOCl, in particular, is mostly detrimental to their function. However, in some cases, oxidative modifications can also regulate and activate functions of some proteins to help the cell overcome those oxidative stress conditions. Long-established among the oxidative modifications that can lead to protein activation are reversible oxidations of the side chain of cysteines. Prime examples are transcription factors such as OxyR [14,15] or the redox-regulated chaperone Hsp33 [16] in *E. coli*. Both proteins become activated upon the formation of disulfide bonds and, conversely, reduction of these disulfides leads to their inactivation. More recently we discovered that N-chlorination of basic amino acid side chains, such as lysine and arginine, is another *in vivo*-reversible modification that mediates the activation of a chaperone-like holdase function in the bacterial protein RidA. After treatment with HOCl or monochloramine, we observed an approximately 60% reduction in the amino group content accompanied by an increase in RidA's hydrophobicity. Consistent with this finding, mass spectrometry (MS) analysis revealed the presence of multiple chlorinated species [12]. This activation of RidA is independent of the oxidation status of its sole cysteine and is fully reversible by DTT, ascorbic acid, glutathione, and the thioredoxin system.

Other proteins, like the bacterial protein CnoX have been found to use a similar mechanism. After activation with HOCl, CnoX, similar to RidA, turns into an effective chaperone-like holdase that can bind a variety of substrate proteins and prevent their aggregation [17]. Moreover, CnoX has a thioredoxin domain and can protect its substrates from irreversible thiol oxidation by forming mixed disulfides with them [17]. But not only bacterial proteins are affected by N-chlorination: recently we discovered that human plasma proteins, such as human serum albumin, are activated by N-chlorination and act not only as chaperones to protect damaged host proteins but can also activate immune cells promoting their production of ROS [18] and mediating their antigen processing [19].

In this study, we identified the residues facilitating RidA's HOCl-driven activation mechanism. Our data suggest that chlorination of basic amino acids by HOCl is not a process that targets one or two crucial amino acids that act as the "switch" affecting the whole protein. Instead, the N-chlorination of multiple residues changes the electrostatic potential of the molecular surface of RidA allowing it to interact with unfolded substrate proteins.

2. Results

2.1. Direct identification of chlorinated sites in RidA after treatment with HOCl revealed chlorination of one arginine and two tyrosines

We previously reported that the enamine/imine deaminase RidA from *E. coli* turns into a potent protein holdase upon N-chlorination of its lysine and arginine residues. RidA, modified in this way (RidA_{HOCl}), can protect other cellular proteins from unfolding due to chlorine stress. Previous mass spectrometric analysis of undigested HOCl-treated RidA showed that the reversible addition of at least 7 and up to 10 chlorine atoms to amino acid residues is concomitant with chaperone-like holdase activity in this protein [12]. However, it remains unknown, which

residues are modified and which of those are required for activation. If we consider arginine, histidine, and lysine as potential targets for a reversible N-chlorination, RidA has 15 possible N-chlorination sites: 5 arginines, 1 histidine, 8 lysines, and the protein's N-terminus (Fig. 1).

To elucidate which amino acids are affected by chlorination, we first performed a mass spectrometric analysis of N-chlorinated RidA after proteolytic digest, specifically searching for peptides having an added mass due to chlorination. Among the above-mentioned 15 possible N-chlorination sites, we were only able to identify R51 to be chlorinated in any of the three replicates after digest with trypsin (Table 1, Fig. 2). The monoisotopic mass of the chlorinated peptide containing R51 was ~ 33.96 Da heavier than the unmodified peptide, corresponding to the monoisotopic mass of a chlorine atom minus the monoisotopic mass of the hydrogen atom it replaced. The same tell-tale mass difference could be observed in 9 fragment γ -ions containing R51 (Fig. 2C). Additionally, we found two chlorinated peptides containing the two tyrosines present in RidA (Y17, Y91) (Table 1). Tyrosine chlorination by HOCl is an irreversible modification that occurs with a much slower rate than the chlorination of lysine, histidine and arginine [9]. But once formed, chlorotyrosine is highly stable [20,21]. Our previous experiments showed that the 7 to 10 added chlorine atoms observed in full-length MS are virtually all removable by DTT, inconsistent with chlorinated tyrosine residues. We thus concluded that our finding is, due to the high stability of the modification in question, probably of auxiliary nature with no functional relevance.

We suspected that the low number of identified N-chlorinated residues in our experiment could be caused by our use of trypsin. Trypsin, the protease most commonly used for the MS analysis of proteins, cleaves proteins after lysine and arginine, the very residues which we suspected to be modified by HOCl. As chlorination of these residues might interfere with trypsin's ability to recognize them, we additionally prepared a digest with chymotrypsin. Nevertheless, we were still not able to detect more N-chlorinated residues in our chymotryptic digest in any replicate but only re-identified chlorinated tyrosines Y17 and Y91 (Table 1).

2.2. DANSO₂H, a novel proteomic probe for N-chlorinated lysine residues in RidA_{HOCl}

Our previous results showed that at least seven and up to ten residues become N-chlorinated in RidA, when it is active as a chaperone. Thus, we were dissatisfied with our limited ability to detect N-chlorinated amino acids using mass spectrometry of proteolytic digests of HOCl-treated RidA. This inability might be due to the inherent instability and high reactivity of N-chloramines. Therefore, we devised a way to stably modify N-chlorinated amino acids.

To this end we utilized dansyl sulfinic acid (5-(dimethylamino)naphthalene-1-sulfinic acid, DANSO₂H), a derivative of the well-characterized reagent dansyl chloride (5-(dimethylamino)naphthalene-1-sulfonyl chloride, DANSCI), which has been used for a long time to derivatize amines, amino acids, and proteins. It reacts with free amino groups and forms stable, highly fluorescent sulfonamides, that can be separated by HPLC and detected by mass spectrometry. In proteins, DANSCI usually reacts only with the free amino group of lysine and the N-terminus [24] (Fig. 3A). Unlike DANSCI, DANSO₂H is not reactive towards unmodified amino groups. Instead, it reacts with monochloramines, forming the same sulfonamide product as the reaction of DANSCI with corresponding unmodified amines (Fig. 3C). This provides

```

1    MSKTIATENAPAAIGPYVQGVDLGNMIITSGQIPVNPKTGEVPADVAAQA
51   RQSLDNVKAIVEAAGLKVGDIVKTTVFVKDLNDFATVNATYEAFFTEHNA
101  TFPARSCVEVARLPKDKVIEIEIAIVRR

```

Fig. 1. The amino acid sequence of the *E. coli* protein RidA (Uniprot entry number: P0AF93). Lysines (K) are highlighted in pink, arginines (R) in purple, and histidine (H) in blue. (For interpretation of the references to color in this figure legend, the reader is referred to the Web version of this article.)

Table 1

Retention times (RT) and properties of unchlorinated and chlorinated peptides identified by LC-MS/MS after tryptic or chymotryptic digest of HOCl-treated RidA. Methionine sulfoxidation is denoted as M_{ox}, and possible sites of chlorination are denoted as R_{Cl} and Y_{Cl} respectively. The PEP-score (posterior error probability) calculated by MaxQuant indicates the probability that a peptide was falsely identified [22,23].

Protease	Residues	Peptide sequence	Unchlorinated			Chlorinated		
			<i>m/z</i> , charge	RT, min	PEP-score	<i>m/z</i> , charge	RT, min	PEP-score
Trypsin	4–38	TIATENAPAAIGPY _{Cl} VQGVDL-GNM _{ox} IITSGQIPVNK	1189.29, +3	47.17	8.21×10^{-72}	1200.95, +3	49.29	4.28×10^{-47}
Trypsin	39–51	TGEVPADVAAQAR _{Cl}	642.83, +2	25.88	4.31×10^{-257}	659.81, +2	26.36	1.81×10^{-5}
Trypsin	80–105	TTVFVKDLNDFATV _{Cl} NATY _{Cl} -EAF _{Cl} FTEHNATFFPAR	910.12, +4	45.45	5.45×10^{-20}	918.68, +4	48.90	1.62×10^{-6}
Chymotrypsin	2–19	SKTIATENAPAAIGPY _{Cl}	802.42, +2	31.27	8.66×10^{-250}	819.40, +2	32.81	3.73×10^{-222}
Chymotrypsin	78–91	VKDLNDFATV _{Cl} NATY _{Cl}	785.89, +2	39.82	1.24×10^{-290}	802.87, +2	39.10	2.67×10^{-148}

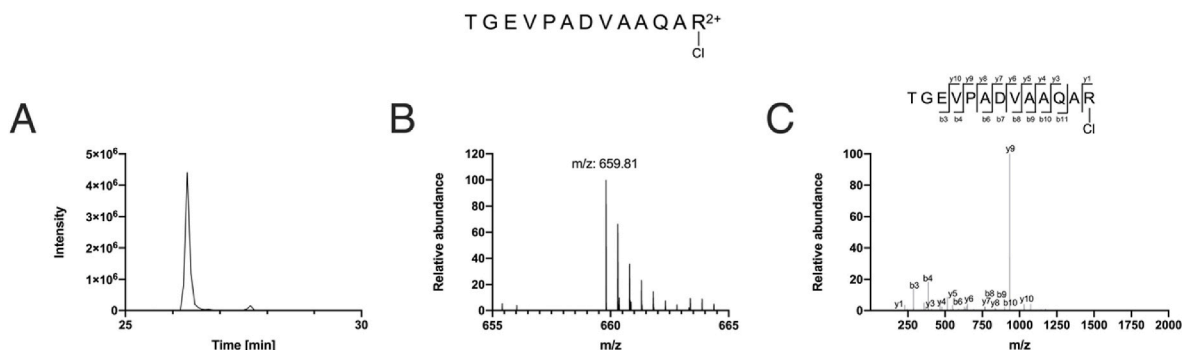


Fig. 2. Arginine R51 is chlorinated upon treatment with HOCl. (A) Extracted ion chromatogram (XIC) of *m/z* 659.81, corresponding to the doubly charged ion of the N-chlorinated peptide TGEVPADVAAQAR₅₁ at a retention time from 25 to 30 min of a tryptic digest of RidA treated with a 10-fold molar excess of HOCl for 10 min at 30 °C. A digest of untreated RidA produces no ion with the respective *m/z* (data not shown). (B) Primary MS spectrum of the N-chlorinated arginine-containing peptide TGEVPADVAAQAR₅₁. (C) Corresponding fragment spectrum of the N-chlorinated peptide contains signals corresponding to 9 y-ions containing the chlorine atom.

us with a method for the selective labeling of N-chlorinated lysine residues. DANSO₂H was synthesized from DANSCl by a reaction with sodium sulfite [25]. The synthesized molecule had a purity of 95%. The only contamination present was dansyl sulfonic acid (DANSO₃H) (Fig. S1), which is chemically inert and reacts neither with amino groups nor N-chlorinated residues [25]. The synthesized DANSO₂H was then used to modify RidA_{HOCl}. DANSCl was used as a positive control to modify untreated RidA (RidA_{UT}), and, as a negative control, DANSO₂H was incubated with RidA_{UT}. As expected, after treatment with DANSCl, RidA_{UT} showed the typical fluorescence of dansyl-modified proteins (Fig. 3B). The same fluorescence albeit to a lesser extent was observed in DANSO₂H-treated RidA_{HOCl} (Fig. 3D). The ~30% lower fluorescence intensity is consistent with our previous finding that only up to 10 out of 15 potential chlorination sites are chlorinated in fully active RidA_{HOCl}. RidA_{UT} treated with DANSO₂H showed virtually no fluorescence, demonstrating the specificity of our probe (Fig. 3D).

2.3. N-chlorinated lysines can be identified after labeling of RidA_{HOCl} with DANSO₂H

Since the fluorescence spectroscopic experiments showed promising results, we then digested the DANSO₂H-treated RidA_{HOCl} with chymotrypsin and performed LC-MS/MS analysis. In total, six lysines (K3, K38, K67, K79, K115, K118) were consistently identified as dansylated in all tested samples of DANSO₂H-treated RidA_{HOCl} (Table 2). Masses corresponding to these dansylated peptides were not observed in RidA_{UT}. Unfortunately, arginines seem not to be modified by DANSO₂H, consistent with DANSCl's preference for free amino groups. Dansylated peptides have a mass difference to the unmodified peptide of ~ 233.05 Da, which equals the mass of DANSO₂H minus the monoisotopic mass of two hydrogen atoms. The dansyl-modification changes the chemical property of a peptide making it more hydrophobic, causing it to elute at significantly higher acetonitrile (ACN) concentrations in the LC. For instance, unmodified peptide harboring K3 eluted at approx. 18% ACN,

whereas the corresponding dansyl-modified peptide eluted at approx. 27% ACN (Fig. 4, Table 2).

No dansylated amino acids were found in a RidA_{UT} sample treated with DANSO₂H. With this novel chemoproteomic method we were able to gather direct evidence for the N-chlorination of six lysines in the active RidA_{HOCl} chaperone-like holdase.

2.4. Mutagenesis reveals two arginines that play an important role in RidA's chaperone activity

Since DANSO₂H is most likely not suitable for the detection of N-chlorinated arginine residues, we used a mutagenesis approach to test if individual amino acids have a particular impact on the chaperone function of N-chlorinated RidA. We thus engineered a total of 13 RidA variants with every single lysine or arginine residue exchanged to a serine.

These 13 RidA variants were expressed and purified from *E. coli* BL21 (DE3) and their chaperone activity after treatment with HOCl was then determined. Activity was tested in a 4-fold excess over citrate synthase. The activity of the variants was compared against wild-type RidA_{HOCl} under the same conditions. The activity of most of HOCl-treated mutants was not affected in a significant way by the exchange of a single N-containing amino acid to serine, when compared to HOCl-treated wild-type protein (Fig. 5). However, two variants lacking specific arginines (R105S and R128S) showed a significantly reduced chaperone activity when compared to HOCl-treated wild-type RidA (RidA_{WT}).

2.5. The concomitant exchange of R105 and R128 does not further decrease chaperone activity

Since an exchange of arginine 105 or 128 resulted in decreased chaperone activity, a variant harboring both mutations (R105S_R128S) was constructed to investigate if a synergistic effect can be observed. The variants were then also treated with HOCl and used in an 8-fold excess

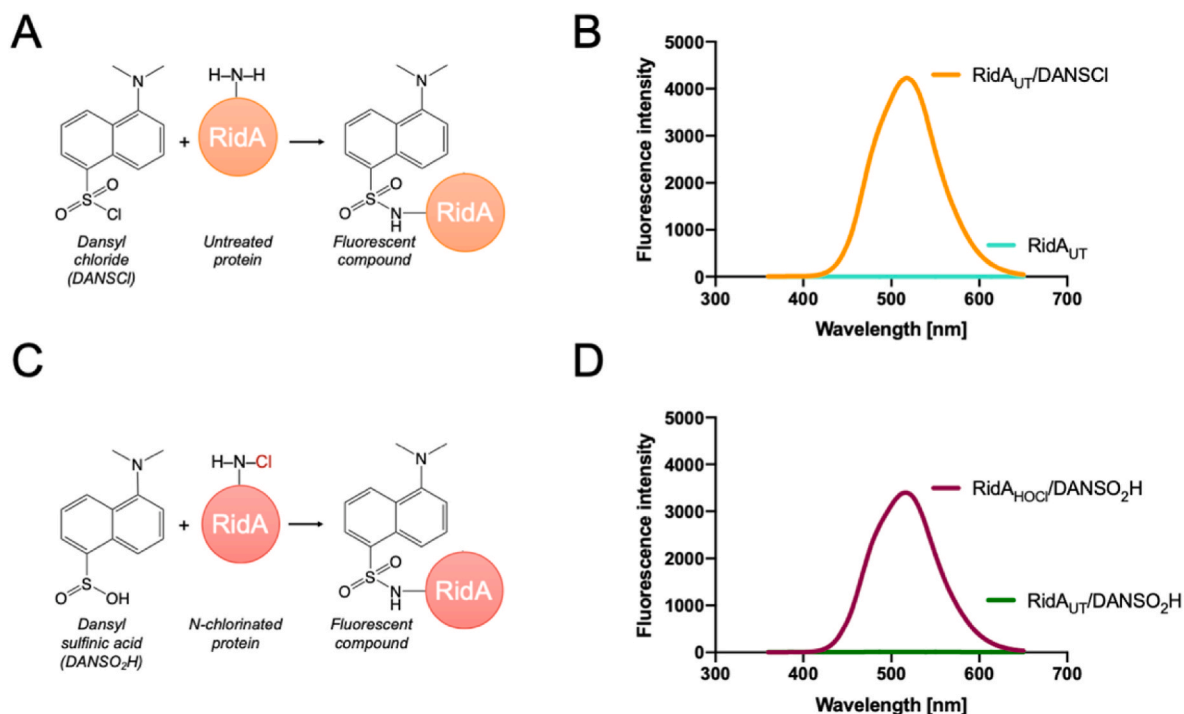


Fig. 3. Modification of RidA with dansyl-derived compounds. (A) Dansyl chloride (DANS-Cl) reacts with an exemplary amino group in RidA forming a “dansylated” fluorescent sulfonamide. (B) Dansylation of proteins can be detected using fluorescence spectroscopy at Ex/Em: 340/500 nm. The reaction of RidA_{UT} with a 10-fold molar excess of DANS-Cl yields a fluorescent protein (orange spectrum), while the protein by itself shows no fluorescence (teal spectrum). (C) Dansyl sulfonic acid (DANSO₂H) is a derivative of DANS-Cl and reacts specifically with N-chlorinated amino groups forming the same “dansylated” fluorescent product found in panel (A). This reaction is thought to proceed via a DAN-Cl intermediate. (D) HOCl-treated RidA (RidA_{HOCl}, RidA treated with a 10-fold molar excess of HOCl for 10 min at 30 °C) reacts with a 10-fold molar excess of DANSO₂H producing a fluorescent peak at the expected excitation/emission wavelengths (purple spectrum). Virtually no fluorescent signal was observed with DANSO₂H-treated RidA_{UT} (green spectrum). (For interpretation of the references to color in this figure legend, the reader is referred to the Web version of this article.)

Table 2

Retention times (RT) and properties of peptides derived from dansyl sulfonic acid (DANSO₂H)-labeling of HOCl-treated RidA after chymotryptic digest and LC-MS/MS. Methionine sulfoxidation and cysteine sulfonic acid modifications are denoted as M_{Ox} and C_{SO₃H} respectively, and lysines that are modified with dansyl sulfonic acid are denoted as K_{DANS}. The PEP-score calculated by MaxQuant indicates the probability that a peptide was falsely identified [22,23].

Protease	Residues	Peptide sequence	Undansylated			Dansylated		
			m/z, charge	RT, min	PEP-score	m/z, charge	RT, min	PEP-score
Chymotrypsin	2–19	SK _{DANS} TIATENAPAAIGPY	802.42, +2	28.57	2.24 × 10 ⁻²⁵⁰	918.95, +2	41.37	1.61 × 10 ⁻²⁵⁰
Chymotrypsin	18–54	VQGVDLGNM _{Ox} ITSGQIPVNP-K _{DANS} TGEVPADVAAQARQSL	1263.99, +3	34.61	5.56 × 10 ⁻⁵⁰	1341.68, +3	41.80	6.63 × 10 ⁻³⁸
Chymotrypsin	67–77	K _{DANS} VGDIVKTTVF	603.86, +2	30.89	5.73 × 10 ⁻¹³	720.38, +2	41.49	2.26 × 10 ⁻⁸
Chymotrypsin	78–91	VK _{DANS} DLNDFATVNTATY	785.89, +2	33.37	8.66 × 10 ⁻¹³⁶	902.42, +2	42.05	6.52 × 10 ⁻¹⁴⁸
Chymotrypsin	103–128	PARSC _{SO₃H} VEVARLPK _{DANS} D-VK _{DANS} EIEIAIVRR	989.56, +3	28.90	1.02 × 10 ⁻⁴⁶	1144.92, +3	43.91	2.28 × 10 ⁻¹⁰

over citrate synthase. However, the chaperone activity of the variant R105S_R128S remained at approximately the same level as the single exchange variants and a further decrease of chaperone activity was not observed (Fig. 6).

2.6. The activation of RidA’s chaperone-like holdase function depends on an overall change of the molecules electrostatic surface

Summed up, our proteomic, chemo-proteomic and mutagenesis studies suggest that no single amino acid acts as a discrete “switch”, but rather the modification of multiple N-containing amino acids leads to the activation of RidA’s chaperone-like holdase function. Even arginines 105 and 128, whose individual exchanges to the inert amino acid serine had the largest effect on activatability, did not show synergistic effects when both were removed. Chaperones are known for surface patches

that enable them to interact with hydrophobic regions of unfolded proteins. Indeed, our previous experiments showed that RidA_{HOCl} did bind a hydrophobic dye much better than RidA_{UT} [12]. In order to understand how N-chlorination of basic amino acids changes the surface properties of RidA, we predicted the electrostatic surface potential of RidA, using the known X-Ray structure of RidA [26] (Fig. 7A). We then computationally substituted lysine and arginine residues with their chlorinated counterparts within the structure data set. Using a customized force field, we were then able to predict the electrostatic surface potential of an N-chlorinated RidA molecule as well (Fig. 7B). Strikingly, the electrostatic surface potential shifted towards a more negative potential, more or less over the complete surface of the molecule. We thus concluded that the loss of positive electrostatic surface potential is the underlying molecular reason for RidA_{HOCl}’s chaperone-like properties.

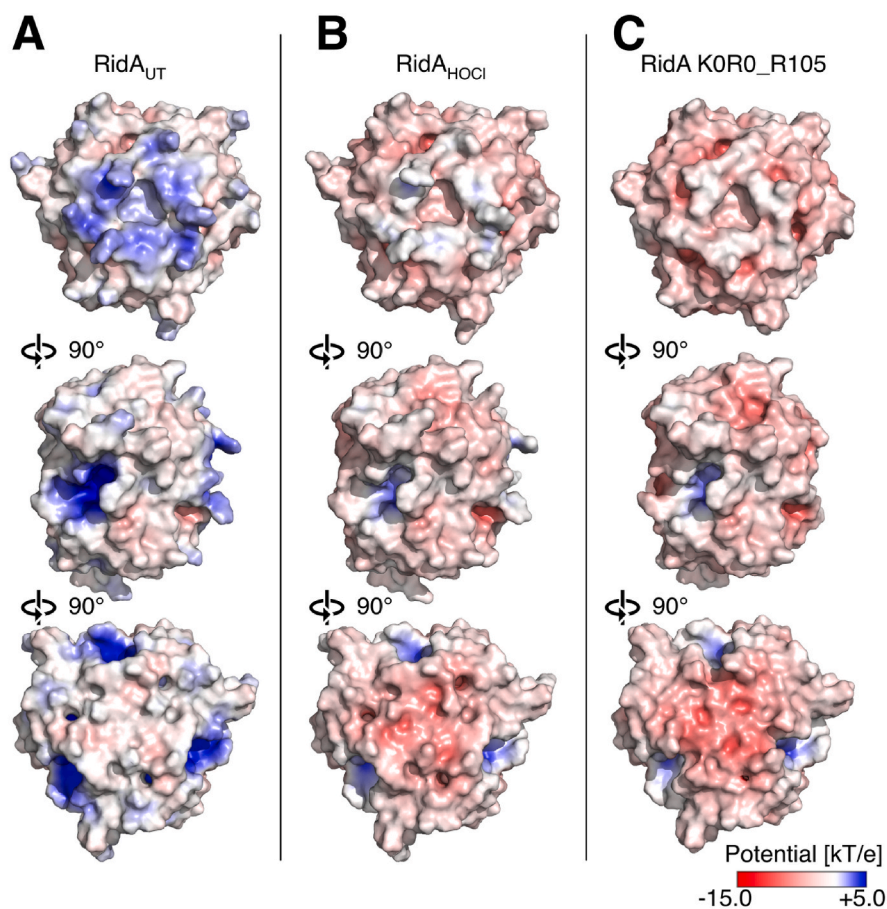


Fig. 7. Calculated electrostatic surface potentials of *E. coli* RidA_{UT} (Uniprot entry: P0AF93, PDB entry: 1QU9), RidA_{HOCl}, and the KOR0_R105 variant. The C-terminal R128 was added to the RidA structure, as it was only partially resolved in the crystal structure. (A) Electrostatic surface visualization of wild-type RidA. The calculation was performed using the Advanced Poisson-Boltzmann Solver in PyMOL using the AMBER force field, as described in the materials and methods section. The coloring scale was chosen from -15 to +5 kT/e according to the legend. Middle panel: the molecule was rotated 90° around the x-axis in comparison to the upper panel. Lower panel: the molecule was rotated 90 more degrees around the x-axis. (B) Electrostatic surface visualization of RidA_{HOCl} using PyMOL. The charge-bearing proton was removed from all lysine and arginine residues, except for R105, and one of the hydrogens was then replaced by a chlorine atom using bond geometries derived from model compounds. The force field (partial charges of respective N and Cl atoms as well as the van der Waals radius of Cl) was adjusted accordingly. (C) Electrostatic surface visualization of KOR0_R105. Amino acid exchanges were introduced in RidA's structure using PyMOL's "Mutagenesis" function.

find a suitable amino acid at all positions. This resulted in a variant, which we termed KOR0_R105 (Fig. 8).

The predicted electrostatic surface potential of this KOR0_R105 variant showed a high similarity to the predicted surface potential of N-chlorinated RidA_{HOCl} (Fig. 7C).

The KOR0_R105 variant was then expressed and purified from *E. coli* BL21 (DE3) and its chaperone activity in comparison to RidA_{UT} and RidA_{HOCl} was determined. As predicted, the RidA variant KOR0_R105 showed already potent chaperone-like activity without HOCl pretreatment, and treatment with HOCl did not increase its chaperone activity significantly (Fig. 9A). Overall, the activity of KOR0_R105 was indeed comparable to HOCl-treated RidA, supporting our hypothesis.

As KOR0_R105 had all possible lysine and arginine residues exchanged, we also tried a more minimalistic approach, in which we exchanged only lysines and arginines at positions where we had proof positive for modification from our MS data or saw effects in our mutagenesis study. These variants were termed 6xK0_1xR0 for the "MS-based" variant and 6xK0_2xR0 for the "MS-based and mutagenesis based" variant (ref. to Fig. 8 for sequence information). Both variants had less residues exchanged than the 10 residues, we observed in full-length MS experiments in fully activated RidA_{HOCl}. Consequently, both variants still needed to be exposed to HOCl to become activated as chaperone-like holdases (Fig. 9C – E).

Taken together, our results suggest that chlorination of basic amino acids by HOCl is not a process that targets one or two crucial amino acids that act as a "switch" that affects the whole protein. Instead, the N-chlorination of multiple residues generates a more negatively charged and hydrophobic molecular surface on RidA, allowing for the interaction with unfolded client proteins. This loss of positive surface charge through N-chlorination is a plausible mechanism for the chaperone-like switch that occurs in a growing number of proteins in response to

exposure to HOCl and other reactive chlorine species.

3. Discussion

After reacting with HOCl or monochloramine, RidA turns into a potent chaperone-like holdase that can bind client proteins. The underlying mechanism was proposed to be the N-chlorination of lysine and arginine residues [12]. Since then, several other proteins have been discovered that seem to switch to a chaperone-like function upon N-chlorination of basic amino acids. However, it was still unclear if the chlorination of one or several specific residues is decisive for chaperone activity of RidA or rather a general modification of multiple amino acid side chains that affects the overall surface of the protein.

Four proteinogenic amino acids are known to be prone to chlorination [27]. First, lysines have an amino group on their side chain that can react with HOCl, forming monochloramines. The guanidino group of arginine can also be N-chlorinated. N-chloramines can be effectively reduced by ascorbate. The side chain of histidine can also react with HOCl, forming a short-lived chloramine. Nevertheless, this chloramine has been shown to be more reactive than corresponding chloramines of lysine and arginine. Moreover, it can rapidly transfer chlorine to other amine groups to generate more stable chloramines [28]. Additionally, histidines are typically less abundant in proteins in comparison to lysines and arginines. For instance, RidA has only one histidine. Lastly, tyrosine is known to become chlorinated. However, the chlorination of tyrosine is an irreversible reaction and leads to the formation of 3-chlorotyrosine [9].

It should be noted that a multitude of other, more reactive targets for HOCl are available *in vivo*, namely thiol groups from cysteines in glutathione and proteins, as well as the other sulfur-containing amino acid methionine. As these are oxidized faster by HOCl than the above-

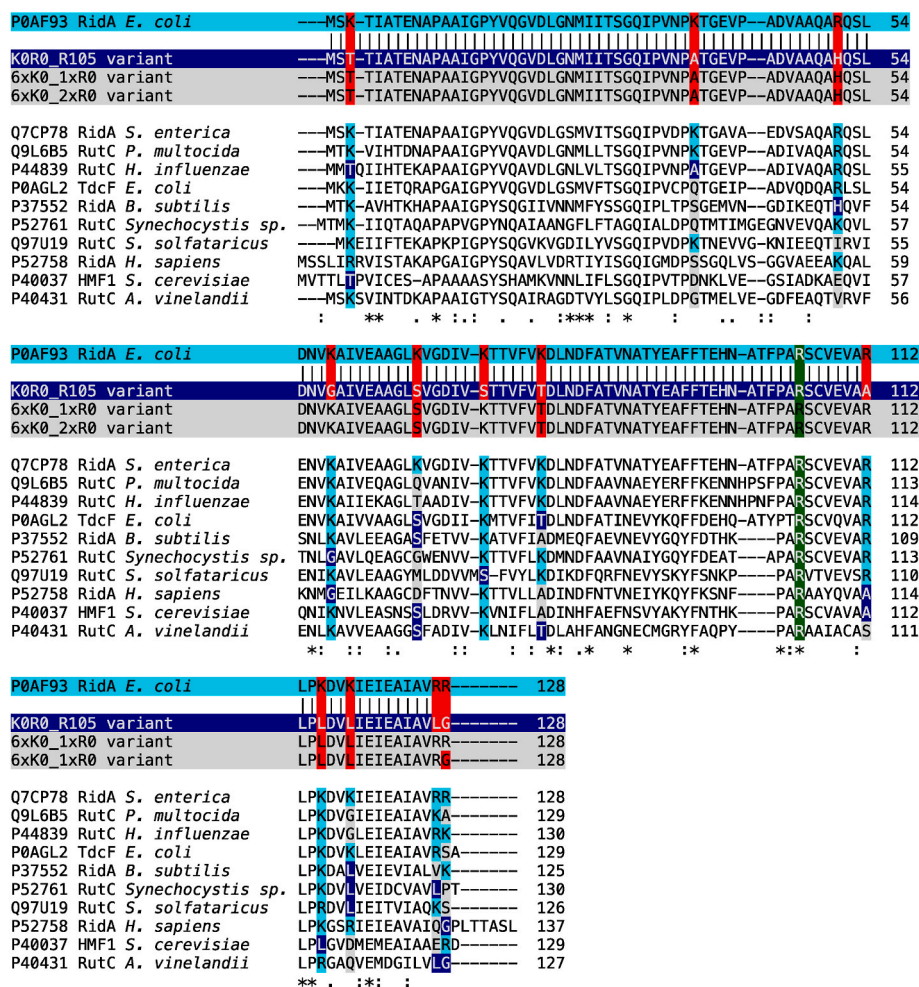


Fig. 8. Sequence alignment of wild-type RidA (P0AF93 RidA *E. coli*) with the K0R0_R105, 6xK0_1xR0, and 6xK0_2xR0 variants and RidA homologs. In the K0R0_R105 variant all lysine and arginine residues were replaced with more electroneutral residues based on amino acids found at those positions in RidA homologs, with the exception of the active-site arginine R105, where no replacement amino acid was found. In variants 6xK0_1xR0 and 6xK0_2xR0 only residues that were found in our MS-based screening, or in our MS-based screening and our mutagenesis screening, respectively, have been replaced with more electroneutral amino acids, again with the exception of R105. The order of sequences is based on overall amino acid identity, ranging from 93.75% (*S. enterica*) to 42.19% (*A. vinelandii*). Arginine and lysine residues found at the position of the replaced amino acids are highlighted in cyan in the alignment of the homologs, while amino acids chosen for replacement are highlighted in blue. Other amino acids at those positions are highlighted in grey. The invariant arginine R105 is highlighted in green. (For interpretation of the references to color in this figure legend, the reader is referred to the Web version of this article.)

mentioned amino acids are chlorinated, they constitute a sink for HOCl and potentially could even remove the N-chlorination from lysine or arginine. Thus, significant chlorination of amino acids most likely only occurs under patho-physiological conditions in the presence of very high HOCl concentrations, such as they might occur in the phagolysosome of neutrophils (see Refs. [29,30] for recent reviews).

3.1. LC-MS/MS analysis revealed HOCl-modified arginine, along with two modified tyrosines

Previously our laboratory reported that RidA's full chaperone-like activity is coinciding with the addition of up to 10 chlorine atoms. However, the LC-MS/MS analysis of chlorinated RidA after tryptic digest performed in the current study only revealed one N-chlorinated amino acid, arginine R51. There was also mass spectrometric evidence for the chlorination of both tyrosines present in RidA, but, as mentioned above, this modification is irreversible and thus should not account for the reversible activation of RidA's chaperone function. Chlorination of lysine or arginine could interfere with the tryptic digest, as these are the amino acids recognized by this particular protease. However, digest with an alternative protease, chymotrypsin did not reveal additional chlorination sites. Alternatively, N-chlorination might potentially be lost during the process of sample preparation, since the amino acid-derived monochloramines, even though less reactive, retain some of the oxidizing capacity of HOCl and are highly reactive towards oxidizable components of reaction buffers [31,32]. Furthermore, N-chlorinated RidA can potentially react with sulfur-containing amino acids found in the proteases used. Therefore, a direct MS-based identification of

chlorinated residues is challenging and does not result in the identification of all modified residues.

Goemans et al. conducted a similar experiment where they performed a mass spectrometric analysis of chlorinated CnoX, in which chaperone activity is also activated by HOCl. Although they identified at least 8 chlorines added to the protein mass during mass spectrometry of full-length CnoX, only five chlorinated amino acid residues were identified using LC-MS/MS analysis after protease digest, among them no lysine residue, hinting at the challenges involved in identifying this particular N-chlorinated amino acid by direct MS analysis [17].

3.2. Dansyl sulfonic acid can be used to stably modify N-chlorinated lysines

Searching for ways to chemically label N-chlorinated lysine, and thus making it accessible for MS-based analysis, dansyl sulfonic acid (DANSO₂H) caught our attention. It has been previously used to derivatize low molecular weight monochloramines in water and other fluids, allowing for their detection by HPLC [25,33]. We synthesized this probe to label the full-length RidA after its chlorination and found that it exclusively reacts with the HOCl-treated protein. We were able to detect a robust fluorescence signal once N-chlorinated RidA was treated with DANSO₂H, but DANSO₂H did not react with the untreated protein. Therefore, DANSO₂H allowed for the specific labeling of N-chlorinated proteins. Using LC-MS/MS analysis of DANSO₂H-derivatized RidA_{HOCl}, we identified 6 lysine residues that we were not able to detect using a direct MS-based approach. These 6 lysines were identified using stringent criteria: they had to be detected and identified in all three

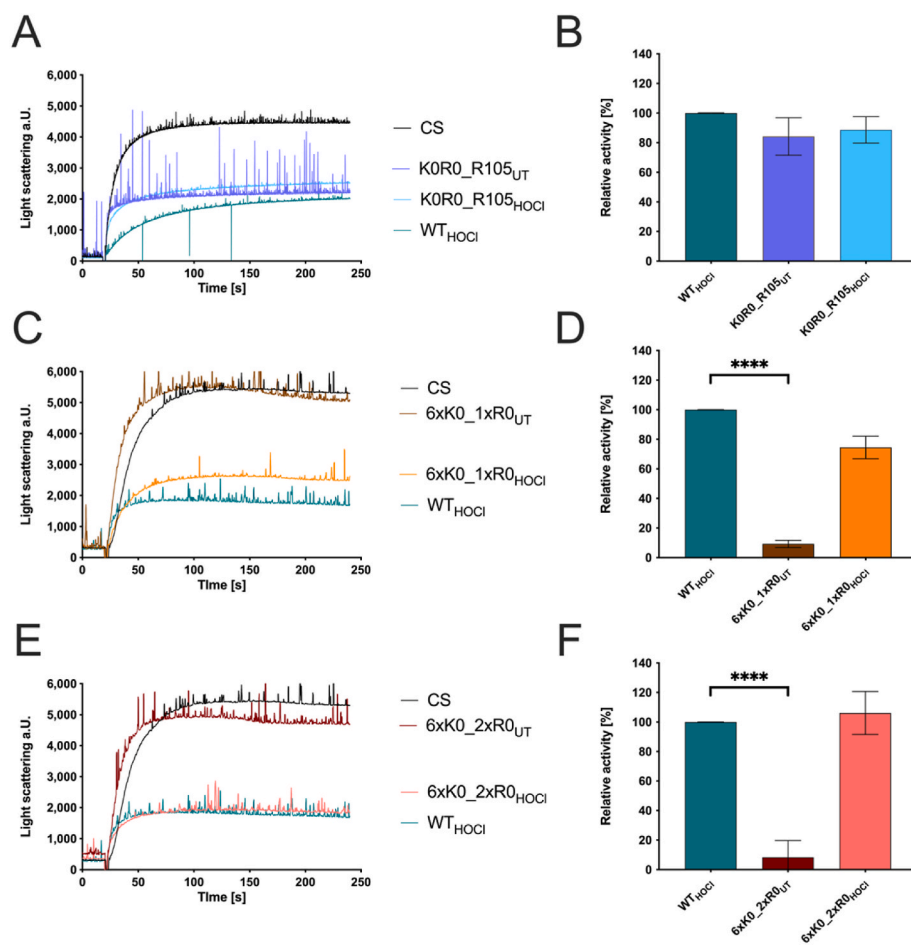


Fig. 9. Chaperone activity of the RidA variants KORO_R105, 6xK0_1xR0 and 6xK0_2xR0. Chaperone activity was tested in an aggregation assay with citrate synthase. (A) HOCl-treated RidA_{WT} (teal) strongly inhibits aggregation of chemically denatured citrate synthase compared to untreated control (black), as measured by light scattering at 360 nm. The variant KORO_R105 (purple) is fully active as a chaperone without any HOCl treatment, and N-chlorination of this variant (light blue) does not influence its chaperone activity. RidA and its variants were N-chlorinated by incubation with a 10-fold molar excess of HOCl for 10 min at 30 °C. (B) Bar graph data represents means and standard deviations of three independent experiments. Difference in chaperone activity between HOCl-treated RidA_{WT} and the untreated and HOCl-treated KORO_R105 was analyzed using a one-way ANOVA with Tukey's comparison test. The activity of RidA_{WT} was set to 100%, and all data are presented in correlation to this control. (C) Variant 6xK0_1xR0 (dark brown) was not active as a chaperone without activation by HOCl. The HOCl-treated variant 6xK0_1xR0_{HOCI} (orange) shows chaperone activity similar to HOCl-treated RidA_{WT} (teal). (D) Bar graph data represents means and standard deviations of three independent experiments. Difference in chaperone activity between was analyzed using a one-way ANOVA with Tukey's comparison test. The activity of RidA_{WT} was set to 100%. (E) Variant 6xK0_2xR0 (dark red) was not active as a chaperone without activation by HOCl. The HOCl-treated variant 6xK0_2xR0_{HOCI} (salmon) shows chaperone activity similar to HOCl-treated RidA_{WT} (teal). (F) Bar graph data represents means and standard deviations of three independent experiments. Difference in chaperone activity between was analyzed using a one-way ANOVA with Tukey's comparison test. The activity of RidA_{WT} was set to 100%. (For interpretation of the references to color in this figure legend, the reader is referred to the Web version of this article.)

experimentally independent replicates of our MS experiments. Using less stringent criteria, we were also able to detect lysines 58 (identified once) and 73 (identified in two of our experiments). Interestingly, the 6 lysine residues we identified consistently are also the lysine residues most exposed to the solvent (Table 3), suggesting they are particularly accessible to HOCl. Nevertheless, chlorine transfer between

Table 3
Accessible surface area and accessibility of lysines and arginines of RidA.
 The analysis was performed using Accessible Surface Area and Accessibility Calculation for Protein (ver. 1.2) (<http://cib.cf.ocha.ac.jp/bitool/ASA/>). "Relative area" is the fraction of the amino acid's total area exposed to the solvent. "Identified by" indicates if these residues were found in the MS-based screening (MS) or in the mutagenesis experiments.

Amino acid position	Amino acid	Area (Å ²)	Relative area (0.0 – 1.0)	Identified by
38	LYS	186.596	0.873	MS
67	LYS	150.440	0.704	MS
115	LYS	146.521	0.686	MS
3	LYS	141.010	0.66	MS
127	ARG	103.542	0.451	-
128	ARG	91.273	0.326	Mutagenesis
79	LYS	83.866	0.392	MS
51	ARG	81.596	0.356	MS
118	LYS	75.743	0.354	MS
112	ARG	67.246	0.293	-
58	LYS	52.885	0.247	-
105	ARG	14.170	0.062	Mutagenesis
73	LYS	9.844	0.046	-

N-chloramines and free amines readily occurs in physiologically relevant amines [34], so we cannot conclude that the identified site of N-chlorination is necessarily the initial site of modification.

DANSO₂H allows for the irreversible derivatization of monochloramines, increasing their stability and simplifying their detection using LC-MS/MS. DANSO₂H initially reacts with monochloramines to form dansyl chloride, which then, in turn, reacts with the newly freed amino group [25,35]. The specificity of this probe in complex samples might be limited due to this issue, as there is a chance that the dansyl chloride diffuses from the originally modified amino residue. The second order rate constant of the reaction of dansyl chloride and the ε-amino group of lysine is 42 M⁻¹ s⁻¹ [36]. Therefore, a two-step procedure with blocking of unmodified amino groups might be considered for complex samples prior to labeling with DANSO₂H.

3.3. Two RidA variants lacking either R105 or R128 showed a significantly decreased chaperone activity

To find out, whether specific amino acids play a key role in the activation of RidA's chaperone-like function, all lysines and arginines were individually changed to serine residues through site-directed mutagenesis. The individual variants were then examined regarding their chaperone activity. The exchange of most lysines and arginines did not affect the chaperone activity of RidA. However, the individual exchange of amino acid residues R105 and R128 resulted in diminished chaperone activity after HOCl treatment. This could indicate that these arginines play a prominent role in chaperone activity.

Potentially, these two arginines are particularly accessible to unfolded proteins in N-chlorinated RidA and, therefore, their chlorination might be important for client protein binding. R128 is the C-terminal amino acid of RidA and, based on structural predictions, exposed to the solvent, which makes it especially accessible to unfolded proteins (Table 3). In the bacterial cytoplasm, RidA is present in the form of a trimer [26] and R128, R127, and K3 of every protein subunit form a large positively charged surface patch (visible in the center of the molecule in the upper panel of Fig. 7A), which is predicted to change to a more electroneutral or even negatively-charged patch after N-chlorination (Fig. 7 B, upper panel) and thus might allow for binding of unfolded client proteins.

The other residue, R105, is highly conserved in three of the seven RidA subfamilies that have enamine/imine deaminase activity [37,38] and was invariable in all RidA homologs that were identified in a blast search in the SwissProt database [39,40] (see also Fig. 8). In *E. coli* and related species, RidA accelerates the release of ammonia from intermediates that result from the dehydration of threonine by IlvA (threonine dehydratase). Arginine 105 plays a particularly important role in the active center of the protein by forming a salt bridge with the carboxylic acid of the substrate [37]. This amino acid is also located in the immediate vicinity of RidA's only cysteine at position 107. This cysteine is redox-sensitive and was modified during the nitrosative stress response (Lindemann et al., 2013). However, the presence of the cysteine is not important for RidA chaperone activity as the mutant lacking the cysteine was as active as wildtype after chlorination [12]. R105, through its position in the active site, is probably also accessible to client proteins, when N-chlorinated.

We also exchanged both arginines R105 and R128 simultaneously through site-directed mutagenesis. If our argumentation that both arginines are of particular importance for client protein binding were true, we would expect the double mutant to be an even less effective chaperone than the individual mutants. Nevertheless, the chaperone activity of this variant corresponded approximately to the chaperone activity of the individual exchanges. One explanation would be the distant localization of these two residues, excluding a mutual influence on chaperone-like activity, even if both residues are absent. Alternatively, the lower chaperone-like activity in both single and double mutants might not be due to the lack of an N-chlorination site but the general structural disturbance that an exchange of these residues (especially in the active site of the protein) induces.

The latter possibility is further supported by the fact that the second-order rate constant of the reaction of HOCl with arginines is three orders of magnitude lower than the one for the reaction with lysines ($k = 7.9 \times 10^3 \text{ M}^{-1} \text{ s}^{-1}$ vs. $k = 26 \text{ M}^{-1} \text{ s}^{-1}$, respectively) [10,41]. Hence, lysines are reacting faster with HOCl than arginines. Nevertheless, it is possible that these two residues are particularly reactive with HOCl. Sometimes particular amino acid residues are more reactive than suggested by the reaction rate with model compounds. As such, cysteines are usually oxidized by H_2O_2 with a second-order rate constant of $k = 14.7 \pm 0.35 \text{ M}^{-1} \text{ s}^{-1}$, while certain cysteines in the active site of peroxiredoxins are oxidized at a much higher velocity ($k = 1.3 \times 10^7 \text{ M}^{-1} \text{ s}^{-1}$) [42]. Therefore, it might be that R105 and R128 in RidA are particularly susceptible to N-chlorination due to the microenvironment in the protein's structure.

3.4. Electrostatic surface modelling of RidA_{HOCl} and the KORO_R105 variant revealed the patterns necessary for RidA's chaperone activity

As shown by our MS-based experiments and our mutagenesis studies, N-chlorination affects multiple basic amino acids (lysines K3, K38, K67, K79, K115, K118 arginine 51 and potentially arginines R105, R128). Therefore, positive charges on the surface of a protein molecule are eliminated, causing an increase in hydrophobicity, which was previously determined experimentally using Nile Red [12,18] and is demonstrated by the calculated electrostatic surface potential of an

N-chlorinated RidA molecule. Protein hydrophobicity as a driving force for chaperone activity is a known mechanism, and other chaperones are also known to have exposed hydrophobic surfaces that allow for the binding of client proteins [43–47]. A rationally designed variant, which mimics the electrostatic surface potential of N-chlorinated RidA and is indeed constitutively active as a chaperone-like holdase, substantiates this hypothesis.

4. Conclusion

For the activation of the chaperone function of RidA, a significant increase in the protein surface hydrophobicity must take place. We present here experimental and computational evidence that this is achieved by reversible N-chlorination of nine individual lysine and arginine residues. The N-chlorination of these basic amino acids removes positive charges from the surface of RidA allowing it to bind and protect unfolded client proteins in the presence of high HOCl concentrations as they appear during inflammatory processes in bacteria-host interactions.

5. Materials and methods

5.1. Preparation of chlorinating agents

The concentration of NaOCl stock was determined spectrophotometrically using a JASCO V-650 UV/VIS spectrophotometer (JASCO, Tokyo, Japan) at 292 nm using the extinction coefficient $\epsilon_{292} = 350 \text{ M}^{-1} \text{ cm}^{-1}$. Monochloramine was prepared freshly by dropwise addition of 200 mM NaOCl solution, dissolved in 0.1 M KOH to 200 mM NH_4Cl solution. After stirring for 5 min, the concentration of the monochloramine produced was measured spectrophotometrically using the extinction coefficient $\epsilon_{242} = 429 \text{ M}^{-1} \text{ cm}^{-1}$.

5.2. Treatment of RidA with HOCl and monochloramine (MCA)

Chlorination of RidA or RidA variants was achieved by adding 10-fold molar excess of HOCl or MCA to the protein solution, a molar excess sufficient to fully activate RidA's chaperone-like function [12]. Samples were incubated for 10 min at 30 °C for HOCl-treatment and 45 min at 37 °C for MCA-treatment. Removal of the residual oxidants was achieved by size-exclusion chromatography using "Micro Bio-Spin P30 Tris Chromatography Columns" (Bio-Rad, München, Germany) or Nap-5 columns (GE Healthcare Life Sciences, Amersham, UK) according to the manufacturer's instructions. Final protein concentrations were determined by measuring the absorbance at 280 nm using a JASCO V-650 UV/VIS spectrophotometer with an extinction coefficient of RidA of $\epsilon_{280} = 2980 \text{ M}^{-1} \text{ cm}^{-1}$.

5.3. Preparation, tryptic and chymotryptic digest of RidA_{HOCl} for mass spectrometry analysis

RidA was treated with HOCl as described above. 5 μl (approx. 25 μg of protein) of untreated and N-chlorinated RidA were mixed together with 35 μl ultrapure water and either 10 μl 5x trypsin digestion buffer (500 mM ammonium bicarbonate, pH 8.0) or 10 μl 5 x chymotrypsin digestion buffer (500 mM Tris-HCl, 10 mM CaCl_2 , pH 8.0). Freshly reconstituted trypsin in 50 mM acetic acid (1 mg/ml) or chymotrypsin in 1 mM HCl (1 mg/ml) was added to the sample for a final 1:20 enzyme-to-protein ratio. The sample was digested at 37 °C for 18 h, and afterwards, the peptides were purified using OMIX C18 tips (Agilent, Santa Clara, CA, USA). Purified peptides were concentrated to dryness and dissolved in 0.1% TFA for LC-MS/MS analysis.

5.4. Peptide cleanup using OMIX C18 tips

The samples after tryptic or chymotryptic digest were first adjusted

to 0.1% (v/v) TFA using 10% TFA solution. Then the tips were first equilibrated 2 times with 100 μ L 100% ACN, followed by 2 times washing with 100 μ L 50% ACN, 0.1% TFA, and lastly 2 times washing with 0.1% TFA. Afterwards, the sample was loaded onto the tip by pipetting it 8 times slowly up and down without releasing the pipette. The tip was then washed 3 times in 500 μ L 0.1% TFA and the sample was eluted in 40 μ L 75% ACN, 0.1% TFA by pipetting it 8 times.

5.5. Liquid chromatography-mass spectrometry (LC-MS/MS)

All MS-based experiments were performed in three experimentally independent replicates. Dansyl-derivatized or unmodified peptides after tryptic or chymotryptic digest were analyzed via LC-MS/MS with an LTQ Orbitrap Elite (Thermo Fisher Scientific, Waltham, MA, USA) as follows: 100 ng of the sample were loaded onto a C18 precolumn (100- μ m \times 2-mm Acclaim PepMap100, 5 μ M, Thermo Fisher Scientific) with 2.5% ACN/0.1% TFA (v/v) at a flow rate of 30 μ L/min for 7 min. The peptides were then loaded onto the main column (75- μ m \times 50-cm Acclaim PepMap100C18, 3 μ m, 100 Å , Thermo Fisher Scientific) with 95% solvent A (0.1% formic acid (v/v)) and 5% solvent B (0.1% formic acid, 84% ACN (v/v)) at a flow rate of 0.4 μ L/min. Peptides were eluted with a linear gradient of 5–40% B (120 min, 0.4 μ L/min). The 20 most intense peaks were selected for MS/MS fragmentation using collision-induced dissociation in the linear ion trap (charge range +2 to +4, exclusion list size: 500, exclusion duration: 35 s, collision energy: 35 eV).

The generated raw files after LC-MS/MS were analyzed using Xcalibur Software (Qual Browser 3.1, Thermo Fischer Scientific, Waltham, MA, USA).

5.6. Mass spectrometry data analysis using MaxQuant

MaxQuant software (version 1.5.1.0, DE) was used to identify and quantify dansyl- and chlorine-modified peptides. The following modifications were added to the variable modification list of the search engine Andromeda: dansylation (+233.05, lysine, arginine, and histidine), chlorination (+33.96, lysine, arginine, histidine, tyrosine) and trioxidation (+47.98, cysteine). For peptide search using Andromeda, the *E. coli* K12 proteome database (taxonomy ID83333) obtained from UniProt (4518 proteins, released September 2019, The UniProt Consortium, 2019) was used. Two miscleavages were allowed, Oxidation (M), Dansylation (KR), Chlorination (KRYH), Carbamidomethyl (C), Trioxidation (C) were chosen as variable modification. Identified peptides were assessed using the “peptides.txt” MaxQuant output file. The availability of modification was monitored using “dansylation-sites.txt”, “chlorination-sites.txt” and “modificationSpecificPeptides.txt” output files. Data was imported and analyzed using Microsoft Excel Version 16.20 (Microsoft, Redmond, WA, USA). All peptide modifications were verified by manual examination of MS/MS spectra using the criteria proposed by Ref. [48]. Described criteria are: 1) identification of unmodified peptide; 2) coverage of modification site by fragment ion series; 3) correct assignment of peaks in MS/MS spectra (neutral losses: Met + O (−64), Met + 2O (−80), Cys + O (−50), Cys + 2O (−66), Cys + 3O (−82)); 4) similar fragmentation patterns between modified and unmodified peptide(s). Residues were considered Dansylated or chlorinated if they were consistently identified as modified in all three replicates. The mass spectrometry proteomics data have been deposited to the ProteomeXchange Consortium via the PRIDE (Perez-Riverol et al., 2019) partner repository with the dataset identifier PXD029595.

5.7. Construction of *RidA* variants with single amino acid substitutions

E. coli strains, plasmids, and primers used in this study are listed in Table 4. The variants KOR0 (a variant that does not contain any of the lysines or arginines of *RidA*), 6xK0_1xR0, and 6xK0_2xR0 were ordered as synthetic genes (Genscript, Piscataway Township, NJ, USA) For the

Table 4

Bacterial strains and plasmids used in this study.

Strain or plasmid	Relevant genotype or description	Source or Reference
<i>Strains</i>		
<i>E. coli</i> XL1 blue	<i>recA1 endA1 gyrA96 thi-1 hsdR17 supE 44 relA1 lac</i>	Stratagene
<i>E. coli</i> BL21 (DE3)	<i>fhuA2 [lon] ompT gal (A DE3) [dcm] ΔhsdS</i>	
<i>E. coli</i> DH5 α	<i>fhuA2 lac(del)U169 phoA glnV44 ϕ80' lacZ(del)M15 gyrA96 recA1 relA1 endA1 thi-1 hsdR17</i>	lab collection
<i>Plasmids</i>		
pUC19	2686 bp, Amp ^R	
pUC19_ridA	3083 bp, Amp ^R , <i>ridA</i>	[12]
pUC19_ridA_K3S	3083 bp, Amp ^R , <i>ridA_K3S</i>	This work
pUC19_ridA_K38S	3083 bp, Amp ^R , <i>ridA_K38S</i>	This work
pUC19_ridA_R51S	3083 bp, Amp ^R , <i>ridA_R51S</i>	This work
pUC19_ridA_K58S	3083 bp, Amp ^R , <i>ridA_K58S</i>	This work
pUC19_ridA_K67S	3083 bp, Amp ^R , <i>ridA_K67S</i>	This work
pUC19_ridA_K73S	3083 bp, Amp ^R , <i>ridA_K73S</i>	This work
pUC19_ridA_K79S	3083 bp, Amp ^R , <i>ridA_K79S</i>	This work
pUC19_ridA_R105S	3083 bp, Amp ^R , <i>ridA_R105S</i>	This work
pUC19_ridA_R112S	3083 bp, Amp ^R , <i>ridA_R112S</i>	This work
pUC19_ridA_K115S	3083 bp, Amp ^R , <i>ridA_K115S</i>	This work
pUC19_ridA_K118S	3083 bp, Amp ^R , <i>ridA_K118S</i>	This work
pUC19_ridA_R127S	3083 bp, Amp ^R , <i>ridA_R127S</i>	This work
pUC19_ridA_R128S	3083 bp, Amp ^R , <i>ridA_R128S</i>	This work
pET22b	5493 bp, Amp ^R , T7-Promotor, HIS ₆ -Tag	Novagen
pET22b_ridA_K3S	5751 bp, Amp ^R , T7-Promotor, HIS ₆ -Tag, <i>ridA_K3S</i>	This work
pET22b_ridA_K38S	5751 bp, Amp ^R , T7-Promotor, HIS ₆ -Tag, <i>ridA_K38S</i>	This work
pET22b_ridA_R51S	5751 bp, Amp ^R , T7-Promotor, HIS ₆ -Tag, <i>ridA_R51S</i>	This work
pET22b_ridA_K58S	5751 bp, Amp ^R , T7-Promotor, HIS ₆ -Tag, <i>ridA_K58S</i>	This work
pET22b_ridA_K67S	5751 bp, Amp ^R , T7-Promotor, HIS ₆ -Tag, <i>ridA_K67S</i>	This work
pET22b_ridA_K73S	5751 bp, Amp ^R , T7-Promotor, HIS ₆ -Tag, <i>ridA_K73S</i>	This work
pET22b_ridA_K79S	5751 bp, Amp ^R , T7-Promotor, HIS ₆ -Tag, <i>ridA_K79S</i>	This work
pET22b_ridA_R105S	5751 bp, Amp ^R , T7-Promotor, HIS ₆ -Tag, <i>ridA_R105S</i>	This work
pET22b_ridA_R112S	5751 bp, Amp ^R , T7-Promotor, HIS ₆ -Tag, <i>ridA_R112S</i>	This work
pET22b_ridA_K115S	5751 bp, Amp ^R , T7-Promotor, HIS ₆ -Tag, <i>ridA_K115S</i>	This work
pET22b_ridA_K118S	5751 bp, Amp ^R , T7-Promotor, HIS ₆ -Tag, <i>ridA_K118S</i>	This work
pET22b_ridA_R127S	5751 bp, Amp ^R , T7-Promotor, HIS ₆ -Tag, <i>ridA_R127S</i>	This work
pET22b_ridA_R128S	5751 bp, Amp ^R , T7-Promotor, HIS ₆ -Tag, <i>ridA_R128S</i>	This work
pUC19_ridA_R105S_R128S	3083 bp, Amp ^R , <i>ridA_R105S_R128S</i>	This work
pET22b_ridA_R105S_R128S	5751 bp, Amp ^R , <i>ridA_R105S_R128S</i>	This work
pEX_ridA_KOR0	2846 bp, Amp ^R , <i>ridA_KOR0</i>	This work
pEX_ridA_KOR0_R105	2846 bp, Amp ^R , <i>ridA_KOR0_R105</i>	This work
pYP169	2622 bp, Kan ^R , <i>lacZ</i>	Y. Pfänder und B. Masepohl, unpublished
pYP169_ridA_KOR0_R105	3019 bp, Kan ^R , <i>lacZ</i> , <i>ridA_KOR0_R105</i>	This work
pET22b_ridA_KOR0_R105	5751 bp, Amp ^R , T7-Promotor, HIS ₆ -Tag, <i>ridA_KOR0_R105</i>	This work
pET22b_ridA_6xK0_2xR0	5751 bp, Amp ^R , T7-Promotor, HIS ₆ -Tag, <i>ridA_6xK0_2xR0</i>	This work
pET22b_ridA_6xK0_1xR0	5751 bp, Amp ^R , T7-Promotor, HIS ₆ -Tag, <i>ridA_6xK0_1xR0</i>	This work

sequence of these variants see Fig. 8, K0R0 has an additional R105S amino acid exchange. Single nucleotides in the *ridA* gene were exchanged using PCR-based mutagenesis, known as QuickChange PCR. PCR was performed using 150 ng of pUC19_riDA (for single amino acid exchanges) or pEX_riDA-K0R0 (to create K0R0_R105) as a template and 125 ng of each specific primer (Table 5) for every single exchange. 20 μ L of the PCR product were digested with 20 U of *DpnI* at 37 °C for 1 h to eliminate the template plasmid. Subsequently, *E. coli* XL-1 blue cells were transformed with the sample using a standard heat-shock method and plated on LB agar plates supplemented with 100 mg/ml ampicillin. Plasmid DNA was isolated from single colonies, and successful mutagenesis was verified by sequencing. Afterwards, *ridA* gene variants were subcloned into pET22b (-) expression vector via the restriction sites *NdeI* and *XhoI*. The resulting pET22b (+)-based constructs were transformed into *E. coli* BL21 (DE3) cells for the subsequent overexpression of RidA variants.

5.8. Overexpression and purification of RidA variants

For overexpression, a single colony of *E. coli* BL21 (DE3) carrying the respective pET22b (+) plasmid was inoculated in 50 mL LB containing 200 mg/L ampicillin and grown overnight at 37 °C, 120 rpm. The next morning, the overnight culture was used to inoculate 5 L of LB medium, supplemented with ampicillin, and incubated at 37 °C and 120 rpm until the OD₆₀₀ reached 0.5–0.6. At this point, protein expression was induced by the addition of 1 mM isopropyl 1-thio- β -D-galactopyranoside (IPTG) to the culture. After 3 h of incubation at 37 °C, 120 rpm, cells were harvested by centrifugation at 7800 \times g and 4 °C for 45 min and either stored at -80 °C or directly used for the purification procedure.

The resulting cell pellet was washed once with lysis buffer (50 mM sodium phosphate, 300 mM NaCl, 10 mM imidazole, pH 8.0) containing 1 ml of EDTA-free protease inhibitor mixture (Roche Applied Science). Cells were disrupted by passing the cell suspension three times through a Constant systems cell disruption system TS benchtop device (Score Group plc, Aberdeenshire, UK) at 1.9 kbar and 4 °C, followed by the addition of PMSF to a final concentration of 1 mM.

Table 5
Primers used in this study.

Primer name	Sequence
K3S_fw	CATATGAGCAGCACTATCGCGACGGAAATGC
K3S_rv	CCGTGCGGATAGTGTCTCATATGTATATCTCCTTC
K38S_fw	CCCGGTAAATCCGAGCAACGGGGGAAGTACC
K38S_rv	GCCCGTGTCTGGGATTTACCGGGATCTGAC
R51S_fw	GCACAGGCAAGCCAGTTCGGTGGATAACG
R51S_rv	CGACTGGCTTGCCTGTGCAGCGACGCTC
K58S_fw	GGATAACGTAAGCGCGATCGTCTGAAGCCGC
K58S_rv	CGACGATCGCGCTTACGTTATCCAGGACTG
K67S_fw	GGCCTGAGCGTGGGCGACATCGTTAAACTACCG
K67S_rv	GTCGCCACGCTCAGGCCAGCGGCTTC
K73S_fw	GGGCGACATCGTTAGCACTACCGTGTGTAATAAG
K73S_rv	CGGTAGTGCTAACGATGTCGCCACTTTCAGG
K79S_fw	CCGTGTTGTAAGCGATCTGAACGACTTCGC
K79S_rv	GATCGCTTACAAACACGGTAGTTTAAACGATGTCGCC
R105S_fw	CCCGGCAAGCTCTTGGCTTGAAGTTGCC
R105S_rv	CGCAAGAGCTTCCGGGGAAGGTGGCG
R112S_fw	GTTGCCAGCCTGCCGAAAGACGTGAAG
R112S_rv	CGGCAGGCTGGCAACTTCAACGCAAG
K115S_fw	CGTCTGCCGAGCGAGTGAAGATTGAGATCG
K115S_rv	CTTACGTCGCTCGGCAGACGGGCAACTTC
K118S_fw	GACGTGAGCATTGAGATCGAAGCGATCGC
K118S_rv	CGATCTCAATGCTACGTCCTTTCGGCAGACG
R127S_fw	CGCTGTTAGCCGCTCGAGCACCACCAC
R127S_rv	CGAGGCGGCTAACACGCGATCGCTTCGATC
R128S_fw	CGCTGTTCTGAGCCTCGAGCACCACCACC
R128S_rv	GCTCGAGGCTACGAACAGCGATCGCTTCG
K0R0_NdeI_fw	CCCATATGAGCACCACACTATCGCGACCG
K0R0_XhoI_rv	GGCTCGAGGCCAGAACACGCGATC
R105_fw	CCTTCCGGCAGCTTCTTGGCTTGAAGTTGCCCG
R105_rv	CAAGAACGTGCCGGGAAGGTGGCGTGTGTTCGG

The cell lysate was centrifuged at 6700 \times g, 4 °C for 1 h, and the supernatant was vacuum filtered through a 0.45 μ m filter. The filtrate was loaded onto a Ni-NTA affinity column. The column was washed with 10 mL washing buffer (50 mM sodium phosphate, 300 mM NaCl, 20 mM imidazole, pH 8.0). For purification of the K0R0_R105 variant, washing buffer was additionally supplemented with 1 M NaCl and 0.1% SDS. Elution was performed using 10 mL elution buffer (50 mM sodium phosphate, 300 mM NaCl, 250 mM imidazole, pH 8.0). Purified proteins were stored at -80 °C and K0R0_R105 was stored at room temperature. Protein concentrations were determined using a JASCO V-650 spectrophotometer using the extinction coefficient $\epsilon_{280} = 2980 \text{ M}^{-1}\text{cm}^{-1}$.

5.9. Protein aggregation assay with citrate synthase

Citrate synthase was chemically denatured in 4.5 M GdnHCl, 40 mM HEPES, pH 7.5 at room temperature overnight. The final concentration of denatured citrate synthase was 12 μ M.

To monitor initial aggregation of citrate synthase, 20 μ L of denatured protein were added to 1580 μ L of 40 mM HEPES, pH 7.5 to a final concentration of 0.15 μ M after 20 s of measurement. To test the chaperone activity, RidA or RidA variants were added prior to the addition of citrate synthase to the buffer at different molar excess (0.5–16-fold) over dimeric citrate synthase. The increase in light scattering was monitored for 240 s using a JASCO FP-8500 fluorescence spectrometer equipped with an EHC-813 temperature-controlled sample holder (JASCO, Tokyo, Japan). Measurement parameters were set to 360 nm (Em/Ex), 30 °C, medium sensitivity, slit width 2.5 nm (Em/Ex). Relative chaperone activity of different RidA variants was calculated based on the difference between initial and final light scattering. The chaperone activity of wild-type chlorinated RidA was set to 100%.

5.10. Synthesis of *N,N*-Dimethyl-1-amino-5-naphthalenesulfonic acid (*Dansyl sulfonic acid*, *DANSO₂H*)

Dansyl sulfonic acid (DANSO₂H) was synthesized from dansyl chloride, as described in Ref. [25] with minor modifications. Dansyl chloride (5 g) was added to a continuously stirred aqueous solution of sodium sulfite (10.7 g in 50 mL) warmed to 70 °C. The reaction temperature was kept at 80 °C for 5 h. After the solution was cooled, DANSO₂H was precipitated from the product mixture by acidifying the solution to pH 4 with concentrated sulfuric acid. The precipitate was then filtered. The precipitate was then dried in a vacuum desiccator over silica gel. The powder was re-dissolved in a cold, aqueous solution of NaOH (2.8 M). The resulting solution was filtered and titrated to pH 4.0 using sulfuric acid. The resulting DANSO₂H was dried again in a vacuum desiccator and stored in the light-protected vial at 4 °C. The purity of the resulting dansyl sulfonic acid (retention time 6.48 min) was confirmed by HPLC (Fig. S1) and was 95%. The 5% contamination by a corresponding sulfonic acid (retention time 6.55 min) does not affect the derivatization of chloramines [25,49].

5.11. Derivatization of RidA with dansyl sulfonic acid and dansyl chloride

200 mM DANSO₂H solution was prepared freshly by dissolving the powder in 200 mM NaHCO₃ buffer, pH 9.0, and 10% (w/w) DANSCI stock solution (370 mM) (abcr, Karlsruhe, Germany) in acetone was directly used.

RidA was chlorinated with HOCl as described above. Using an NAP-5 gel filtration column, residual HOCl was removed, and the buffer was exchanged to 200 mM NaHCO₃ buffer, pH 9.0. 250 μ M RidA_{HOCl} or RidA_{UT} were incubated with a 50-fold molar excess of DANSCI or DANSO₂H for 1 h, 37 °C, 1300 rpm. The derivatizing agent was removed using an NAP-5 gel filtration column. Successful derivatization of RidA by monitoring the fluorescence of the resulting sulfonamide was determined by a fluorescence emission scan from 360 to 600 nm in a JASCO FP-8500 fluorescence spectrometer with the following parameters: 340

nm excitation, 2.5 nm slit width (Ex/Em) and medium sensitivity.

5.12. Preparation and chymotryptic digest of dansylated proteins for mass spectrometry analysis

5 μ L (approx. 8 μ g of protein) of each dansylated sample prepared above were mixed together with 25 μ L ultrapure water and 10 μ L 5 x chymotrypsin digestion buffer (500 mM Tris-HCl, 10 mM CaCl₂, pH 8.0). pH of the resulting solution was monitored to be around 8.0. Then, DTT was added to the solution to a final concentration of 10 mM and incubated at 60 °C for 45 min. After the sample was cooled to room temperature, 3.5 μ L of freshly prepared 500 mM iodoacetamide solution in pure water were added to a final concentration of 20 mM. The sample was incubated at room temperature for 30 min, protected from light. To quench the alkylation reaction, 1 μ L of 500 mM DTT was added, and the volume of the solution was adjusted to 50 μ L using pure water. Chymotrypsin, reconstituted to a concentration of 1 mg/mL in 1 mM HCl, was then added to the sample for a final 1:20 enzyme-to-protein ratio. The reaction mixture was incubated at 37 °C for 18 h. The sample was then desalted using OMIX C18 tips (Agilent, Santa Clara, CA, USA) as described above. Purified peptides were concentrated to dryness and dissolved in 0.1% TFA for LC-MS/MS analysis, performed as described above.

5.13. Protein structure modification and electrostatic surface modelling of RidA, RidA_{HOC} and KOR0_R105

E. coli RidA crystal structure was accessed using PDB entry number 1QU9 and visualized using PyMOL 2.3.4 (Schrödinger, New York, NY, USA). This structure was converted to a PQR file using the PDB2PQR webserver [50] under an assumed pH of 7.0, using PROPKA to assign protonation and the AMBER forcefield to assign partial charges and atomic volumes to the structure's atoms. Using the resulting PQR file as input, PyMOL's APBS plugin was used to calculate the electrostatic surface potential.

To model the N-chlorinated RidA_{HOC}, the PQR file of RidA was manipulated using a custom python script (Supplemental Material S2). This script removes charge bearing protons from specified lysine and arginine residues, rectifies binding angles (in case of deprotonated arginine) and replaces one nitrogen-attached hydrogen atom in these residues with a chlorine atom using the following bond geometries and partial charges: Charge of the chlorine atom: 0.07, charge of the nitrogen atom: -0.61 (based on values for CH₃NHCl [51]), radius of the chlorine atom 1.75 Å [52], length of the N-Cl bond: 1.784 Å (based on values for NH₂Cl [53]). The resulting manipulated PQR file was then used to calculate the electrostatic surface potential of RidA_{HOC} using the APBS plugin of PyMOL.

The structure of RidA variant KOR0_R105 was modeled using the mutagenesis function of PyMOL. The specified amino acids in wild-type RidA were exchanged as follows:

K3 → T3.
K38 → A38.
R51 → H51.
K58 → G58.
K67 → S67.
K73 → S73.
K79 → T79.
R112 → A112.
K115 → L115.
K118 → L118.
R127 → L127.
R128 → G128.

The electrostatic surface potential for this variant was then calculated as outlined for the wildtype above (conversion of the pdb-file to a PQR file using the PDB2PQR webserver under an assumed pH of 7.0, using PROPKA to assign protonation and the AMBER forcefield and

subsequent use of the ABPS plugin in PyMOL).

Author contributions

MV, JF, AM, LIL conceived and designed the study. NL assisted in and performed protein expression and purification experiments. MV performed mass spectrometry and fluorescence spectroscopy experiments and evaluated MS data. MV and LIL synthesized and characterized the DANSO₂H probe. YS and KSC designed and assisted in the synthesis of the DANSO₂H probe. JF designed and performed site directed mutagenesis experiments, mass spectrometry experiments, and citrate synthase aggregation assays. AM designed site directed mutagenesis experiments and the KOR0_R105 variant and performed citrate synthase aggregation assays. KR and BS performed mass spectrometry measurements and assisted in MS data handling. MK, CJ, TJ, EH, JEB consulted on the computational structure prediction and calculation of the electrostatic surface potential of RidA, RidA_{HOC} and KOR0_R105. LIL and MV calculated the electrostatic surface potentials. MV, AM, JF, LIL wrote the manuscript, all other authors consulted on the manuscript.

Declaration of interest

The authors declare that they have no known competing financial interests or personal relationships that could have appeared to influence the work reported in this paper.

Acknowledgments

LIL acknowledges funding from the DFG Priority Program 1710 "Dynamics of Thiol-based Redox Switches in Cellular Physiology" through grant LE2905/1-2. LIL, EH, and JEB would like to thank the DFG Research Training Grant 2341 "Microbial Substrate Conversion" for supporting this work, and JEB further acknowledges funding from the DFG CRC1316-1 and BA 4193/7-1.

Appendix A. Supplementary data

Supplementary data to this article can be found online at <https://doi.org/10.1016/j.redox.2022.102332>.

References

- [1] E. Mortaz, S.D. Alipoor, I.M. Adcock, S. Mumby, L. Koenderman, Update on neutrophil function in severe inflammation, *Front. Immunol.* 9 (2018) 2171, <https://doi.org/10.3389/fimmu.2018.02171>.
- [2] C.C. Winterbourn, A.J. Kettle, M.B. Hampton, Reactive oxygen species and neutrophil function, *Annu. Rev. Biochem.* 85 (2016) 765–792, <https://doi.org/10.1146/annurev-biochem-060815-014442>.
- [3] J.M. Albrich, C.A. McCarthy, J.K. Hurst, Biological reactivity of hypochlorous acid: implications for microbicidal mechanisms of leukocyte myeloperoxidase, *Proc. Natl. Acad. Sci. U.S.A.* 78 (1981) 210–214, <https://doi.org/10.1073/pnas.78.1.210>.
- [4] W.A. Prütz, Hypochlorous acid interactions with thiols, nucleotides, DNA, and other biological substrates, *Arch. Biochem. Biophys.* 332 (1996) 110–120, <https://doi.org/10.1006/abbi.1996.0322>.
- [5] A.C. Carr, J.J.M. Van Den Berg, C.C. Winterbourn, Chlorination of cholesterol in cell membranes by hypochlorous acid, *Arch. Biochem. Biophys.* 332 (1996) 63–69, <https://doi.org/10.1006/abbi.1996.0317>.
- [6] M. Deborde, U. von Gunten, Reactions of chlorine with inorganic and organic compounds during water treatment-Kinetics and mechanisms: a critical review, *Water Res.* 42 (2008) 13–51, <https://doi.org/10.1016/j.watres.2007.07.025>.
- [7] C.C. Winterbourn, J.J.M. van den Berg, E. Roitman, F.A. Kuypers, Chlorohydrin formation from unsaturated fatty acids reacted with hypochlorous acid, *Arch. Biochem. Biophys.* 296 (1992) 547–555, [https://doi.org/10.1016/0003-9861\(92\)90609-Z](https://doi.org/10.1016/0003-9861(92)90609-Z).
- [8] S.E. McGowan, R.J. Thompson, Extracellular matrix proteoglycan degradation by human alveolar macrophages and neutrophils, *J. Appl. Physiol.* 66 (1989) 400–409, <https://doi.org/10.1152/jappl.1989.66.1.400>.
- [9] C.L. Hawkins, D.I. Pattison, M.J. Davies, Hypochlorite-induced oxidation of amino acids, peptides and proteins, *Amino Acids* 25 (2003) 259–274, <https://doi.org/10.1007/s00726-003-0016-x>.
- [10] D.I. Pattison, M.J. Davies, C.L. Hawkins, Reactions and reactivity of myeloperoxidase-derived oxidants: differential biological effects of hypochlorous

- and hypothiocyanous acids, *Free Radic. Res.* 46 (2012) 975–995, <https://doi.org/10.3109/10715762.2012.667566>.
- [11] C.L. Hawkins, M.J. Davies, Hypochlorite-induced oxidation of proteins in plasma: formation of chloramines and nitrogen-centred radicals and their role in protein fragmentation, *Biochem. J.* 340 (1999) 539–548, <https://doi.org/10.1042/0264-6021:3400539>.
- [12] A. Müller, S. Langklotz, N. Lupilova, K. Kuhlmann, J.E. Bandow, L.I.O. Leichert, Activation of RidA chaperone function by N-chlorination, *Nat. Commun.* 5 (2014) 5804, <https://doi.org/10.1038/ncomms5804>.
- [13] J. Winter, M. Ilbert, P.C.F. Graf, D. Özcelik, U. Jakob, Bleach activates a redox-regulated chaperone by oxidative protein unfolding, *Cell* 135 (2008) 691–701, <https://doi.org/10.1016/j.cell.2008.09.024>.
- [14] G. Storz, L.A. Tartaglia, B.N. Ames, Transcriptional regulator of oxidative stress-inducible genes: direct activation by oxidation, *Science* 248 (1990) 189–194, <https://doi.org/10.1126/science.2183352>.
- [15] M. Zheng, F. Åslund, G. Storz, Activation of the OxyR transcription factor by reversible disulfide bond formation, *Science* 279 (1998) 1718–1721, <https://doi.org/10.1126/science.279.5357.1718>.
- [16] U. Jakob, W. Muse, M. Eser, J.C.A. Bardwell, Chaperone activity with a redox switch, *Cell* 96 (1999) 341–352, [https://doi.org/10.1016/S0092-8674\(00\)80547-4](https://doi.org/10.1016/S0092-8674(00)80547-4).
- [17] C.V. Goemans, D. Vertommen, R. Agrebi, J.F. Collet, CnoX is a chaperedoxin: a holdase that protects its substrates from irreversible oxidation, *Mol. Cell* 70 (2018) 614–627, <https://doi.org/10.1016/j.molcel.2018.04.002>.
- [18] A. Ulfing, A.V. Schulz, A. Müller, N. Lupilov, L.I. Leichert, N-chlorination mediates protective and immunomodulatory effects of oxidized human plasma proteins, *Elife* 8 (2019), e47395, <https://doi.org/10.7554/eLife.47395>.
- [19] A. Ulfing, V. Bader, M. Varatnitskaya, N. Lupilov, K.F. Winklhofer, L.I. Leichert, Hypochlorous acid-modified human serum albumin suppresses MHC class II-dependent antigen presentation in pro-inflammatory macrophages, *Redox Biol.* 43 (2021) 101981, <https://doi.org/10.1016/j.redox.2021.101981>.
- [20] I. Hendrikje Buss, R. Senthilmohan, B.A. Darlow, N. Mogridge, A.J. Kettle, C. C. Winterbourn, 3-Chlorotyrosine as a marker of protein damage by myeloperoxidase in tracheal aspirates from preterm infants: association with adverse respiratory outcome, *Pediatr. Res.* 53 (2003) 455–462, <https://doi.org/10.1203/01.PDR.0000050655.25689.CE>.
- [21] C.C. Winterbourn, A.J. Kettle, Biomarkers of myeloperoxidase-derived hypochlorous acid, *Free Radic. Biol. Med.* 29 (2000) 403–409, [https://doi.org/10.1016/S0891-5849\(00\)00204-5](https://doi.org/10.1016/S0891-5849(00)00204-5).
- [22] L. Käll, J.D. Storey, M.J. MacCoss, W.S. Noble, Posterior error probabilities and false discovery rates: two sides of the same coin, *J. Proteome Res.* 7 (2008) 40–44, <https://doi.org/10.1021/pr700739d>.
- [23] J. Cox, M. Mann, MaxQuant enables high peptide identification rates, individualized p.p.b.-range mass accuracies and proteome-wide protein quantification, *Nat. Biotechnol.* 26 (2008) 1367–1372, <https://doi.org/10.1038/nbt.1511>.
- [24] W.T. Hsieh, K.S. Matthews, Lactose repressor protein modified with dansyl chloride: activity effects and fluorescence properties, *Biochemistry* 24 (1985) 3043–3049, <https://doi.org/10.1021/bi00333a036>.
- [25] F.E. Scully, J.P. Yang, K. Mazlina, F. Bernard Daniel, Derivatization of organic and inorganic N-chloramines for high-performance liquid chromatographic analysis of chlorinated water, *Environ. Sci. Technol.* 18 (1984) 787–792, <https://doi.org/10.1021/es00128a012>.
- [26] K. Volz, A test case for structure-based functional assignment: the 1.2 Å crystal structure of the yjgF gene product from *Escherichia coli*, *Protein Sci.* 8 (2008) 2428–2437, <https://doi.org/10.1110/ps.8.11.2428>.
- [27] A.V. Peskin, C.C. Winterbourn, Kinetics of the reactions of hypochlorous acid and amino acid chloramines with thiols, methionine, and ascorbate, *Free Radic. Biol. Med.* 30 (2001) 572–579, [https://doi.org/10.1016/S0891-5849\(00\)00506-2](https://doi.org/10.1016/S0891-5849(00)00506-2).
- [28] D.I. Pattison, M.J. Davies, Kinetic analysis of the role of histidine chloramines in hypochlorous acid mediated protein oxidation, *Biochemistry* 44 (2005) 7378–7387, <https://doi.org/10.1021/bi0474665>.
- [29] A. Ulfing, L.I. Leichert, The effects of neutrophil-generated hypochlorous acid and other hypohalous acids on host and pathogens, *Cell. Mol. Life Sci.* 78 (2) (2021) 385–414, <https://doi.org/10.1007/s00018-020-03591-y>.
- [30] M. Varatnitskaya, A. Degrossoli, L.I. Leichert, Redox regulation in host-pathogen interactions: thiol switches and beyond, *Biol. Chem.* 402 (3) (2020) 299–316, <https://doi.org/10.1515/hsz-2020-0264>.
- [31] L.V. Ashby, R. Springer, M.B. Hampton, A.J. Kettle, C.C. Winterbourn, Evaluating the bactericidal action of hypochlorous acid in culture media, *Free Radic. Biol. Med.* 159 (2020) 119–124, <https://doi.org/10.1016/j.freeradbiomed.2020.07.033>.
- [32] D. Pattison, M. Davies, Reactions of myeloperoxidase-derived oxidants with biological substrates: gaining chemical insight into human inflammatory diseases, *Curr. Med. Chem.* 13 (2006) 3271–3290, <https://doi.org/10.2174/092986706778773095>.
- [33] F.E. Scully, K. Mazina, D. Sonenshine, F. Kopfler, Quantitation and identification of organic N-chloramines formed in stomach fluid on ingestion of aqueous hypochlorite, *Environ. Health Perspect.* 69 (1986) 259–265, <https://doi.org/10.2307/3430395>.
- [34] A.V. Peskin, R.G. Midwinter, D.T. Harwood, C.C. Winterbourn, Chlorine transfer between glycine, taurine, and histamine: reaction rates and impact on cellular reactivity, *Free Radic. Biol. Med.* 38 (3) (2004) 397–405, <https://doi.org/10.1016/j.freeradbiomed.2004.11.006>.
- [35] J.A. Jersey, E. Choshen, J.N. Jensen, J.D. Johnson, F.E. Scully, N-chloramine derivatization mechanism with dansylsulfonic acid: yields and routes of reaction, *Environ. Sci. Technol.* 24 (1990) 1536–1541, <https://doi.org/10.1021/es00080a013>.
- [36] W.R. Gray, [12] Dansyl chloride procedure, *Methods Enzymol.* 11 (1967) 139–151, [https://doi.org/10.1016/S0076-6879\(67\)11014-8](https://doi.org/10.1016/S0076-6879(67)11014-8).
- [37] J.A. Lambrecht, J.M. Flynn, D.M. Downs, Conserved YjgF protein family deaminates reactive enamine/imine intermediates of pyridoxal 5'-phosphate (PLP)-dependent enzyme reactions, *J. Biol. Chem.* 287 (2012) 3454–3461, <https://doi.org/10.1074/jbc.M111.304477>.
- [38] X. Liu, J. Zeng, X. Chen, W. Xie, Crystal structures of RidA, an important enzyme for the prevention of toxic side products, *Sci. Rep.* 6 (2016), <https://doi.org/10.1038/srep30494>.
- [39] S.F. Altschul, W. Gish, W. Miller, E.W. Myers, D.J. Lipman, Basic local alignment search tool, *J. Mol. Biol.* 215 (1990) 403–410, [https://doi.org/10.1016/S0022-2836\(05\)80360-2](https://doi.org/10.1016/S0022-2836(05)80360-2).
- [40] A. Bateman, M.J. Martin, S. Orchard, M. Magrane, R. Agivetova, S. Ahmad, E. Alpi, E.H. Bowler-Barnett, R. Britto, B. Bursteinas, H. Bye-A-Jee, R. Coetzee, A. Cukura, A. Da Silva, P. Denny, T. Dogan, T.G. Ebenezzer, J. Fan, L.G. Castro, P. Garmiri, G. Georgiou, L. Gonzales, E. Hatton-Ellis, A. Hussein, A. Ignatchenko, G. Insana, R. Ishtiaq, P. Jokinen, V. Joshi, D. Jyothi, A. Lock, R. Lopez, A. Luciani, J. Luo, Y. Lussi, A. MacDougall, F. Madeira, M. Mahmoudy, M. Menchi, A. Mishra, K. Moulang, A. Nightingale, C.S. Oliveira, S. Pundir, G. Qi, S. Raj, D. Rice, M. R. Lopez, R. Saidi, J. Sampson, T. Sawford, E. Speretta, E. Turner, N. Tyagi, P. Vasudev, V. Volynkin, K. Warner, X. Watkins, R. Zaru, H. Zellner, A. Bridge, S. Poux, N. Redaschi, L. Aimo, G. Argoud-Puy, A. Auchincloss, K. Axelsen, P. Bansal, D. Baratin, M.C. Blatter, J. Bolleman, E. Boutet, L. Breuzia, C. Casals-Casas, E. de Castro, K.C. Echiouk, E. Couderb, B. Cuche, M. Doche, D. Dornevil, A. Estreicher, M.L. Famiglietti, M. Feuermann, E. Geateiger, S. Gehant, V. Gerritsen, A. Gos, N. Gruaz-Gumowski, U. Hinz, C. Hulo, N. Hyka-Nouspikel, F. Jungo, G. Keller, A. Kerhornou, V. Lara, P. Le Mercier, D. Lieberherr, T. Lombardot, et al., UniProt: the universal protein knowledgebase in 2021, *Nucleic Acids Res.* 49 (2021) D480–D489, <https://doi.org/10.1093/nar/gkaa1100>.
- [41] D.I. Pattison, M.J. Davies, Absolute rate constants for the reaction of hypochlorous acid with protein side chains and peptide bonds, *Chem. Res. Toxicol.* 14 (2001) 1453–1464, <https://doi.org/10.1021/tx0155451>.
- [42] A.V. Peskin, F.M. Low, L.N. Paton, G.J. Maghzal, M.B. Hampton, C.C. Winterbourn, The high reactivity of peroxiredoxin 2 with H₂O₂ is not reflected in its reaction with other oxidants and thiol reagents, *J. Biol. Chem.* 282 (2007) 11885–11892, <https://doi.org/10.1074/jbc.M700339200>.
- [43] P.C.F. Graf, M. Martinez-Yamout, S. VanHaerents, H. Lillie, H.J. Dyson, U. Jakob, Activation of the redox-regulated chaperone Hsp33 by domain unfolding, *J. Biol. Chem.* 279 (2004) 20529–20538, <https://doi.org/10.1074/jbc.M401764200>.
- [44] P. Koldewey, F. Stull, S. Horowitz, R. Martin, J.C.A.B. Correspondence, Forces driving chaperone action in brief, *Cell* 166 (2016) 369–379, <https://doi.org/10.1016/j.cell.2016.05.054>.
- [45] P. Koldewey, S. Horowitz, J.C.A. Bardwell, Chaperone-client interactions: non-specificity engenders multifunctionality, *J. Biol. Chem.* 292 (2017) 12010–12017, <https://doi.org/10.1074/jbc.R117.796862>.
- [46] M.S. Kumar, M. Kapoor, S. Sinha, G.B. Reddy, Insights into hydrophobicity and the chaperone-like function of α -A- and α B-crystallins: an isothermal titration calorimetric study, *J. Biol. Chem.* 280 (2005) 21726–21730, <https://doi.org/10.1074/jbc.M500405200>.
- [47] M.P. Mayer, B. Bukau, Hsp 70 chaperones: cellular functions and molecular mechanism, *Cell. Mol. Life Sci.* 62 (2005) 670–684, <https://doi.org/10.1007/s00018-004-4464-6>.
- [48] T. Nybo, H. Cai, C.Y. Chuang, L.F. Gamon, A. Rogowska-Wrzesinska, M.J. Davies, Chlorination and oxidation of human plasma fibronectin by myeloperoxidase-derived oxidants, and its consequences for smooth muscle cell function, *Redox Biol.* 19 (2018) 388–400, <https://doi.org/10.1016/j.redox.2018.09.005>.
- [49] A. Alpmann, G. Morlock, Rapid and sensitive determination of acrylamide in drinking water by planar chromatography and fluorescence detection after derivatization with dansylsulfonic acid, *J. Separ. Sci.* 31 (2008) 71–77, <https://doi.org/10.1002/jssc.200700391>.
- [50] E. Jurrus, D. Engel, K. Star, K. Monson, J. Brandi, L.E. Felberg, D.H. Brookes, L. Wilson, J. Chen, K. Liles, M. Chun, P. Li, D.W. Gohara, T. Dolinsky, R. Konecny, D.R. Koes, J.E. Nielsen, T. Head-Gordon, W. Geng, R. Krasny, G.W. Wei, M.J. Holst, J.A. McCammon, N.A. Baker, Improvements to the APBS biomolecular solvation software suite, *Protein Sci.* 27 (2018) 112–128, <https://doi.org/10.1002/pro.3280>.
- [51] M.B. Heeb, I. Kristiana, D. Trogolo, J.S. Arey, U. von Gunten, Formation and reactivity of inorganic and organic chloramines and bromamines during oxidative water treatment, *Water Res.* 110 (2017) 91–101, <https://doi.org/10.1016/j.watres.2016.11.065>.
- [52] A. Bondi, Van der waals volumes and radii, *J. Phys. Chem.* 68 (1964) 441–451, <https://doi.org/10.1021/j100785a001>.
- [53] M.D. Harmony, V.W. Laurie, R.L. Kuczkowski, R.H. Schwendeman, D.A. Ramsay, F. J. Lovas, W.J. Lafferty, A.G. Maki, Molecular structures of gas phase polyatomic molecules determined by spectroscopic methods, *J. Phys. Chem. Ref. Data* 8 (1979) 619–722, <https://doi.org/10.1063/1.555605>.